Observational Study

Medicine®

OPEN

Craniocervical computed tomography angiography with adaptive iterative dose reduction 3D algorithm and automatic tube current modulation in patients with different body mass indexes

Shujing Yu, BS*, Jing Zheng, MD, Li Zhang, MD

Abstract

The aim of this study was to investigate the feasibility of head and neck computed tomography angiography (CTA) using the 80-kV tube voltage and the adaptive iterative dose reduction (AIDR) 3D algorithm in patients with different body mass indexes (BMIs).

From November 2016 to January 2017, 128 consecutive patients scheduled for head and neck CTA examinations were randomized into the 100-kV group (n = 60) and the 80-kV group (n = 68). Both groups used the automatic tube current modulation technique and the AIDR 3D algorithm. The patients were further grouped as slender (BMI < 22 kg/m^2), normal weight (22 kg/m^2 ≤ BMI < 25 kg/m^2), and overweight (BMI ≥ 25 kg/m^2). The image quality and the radiation dose of each subgroup were analyzed.

The images of the head and neck vessels and the brain tissue obtained with 100 kV were all of diagnostic quality. Slender and normal weight patients imaged with 80 kV also produced images of diagnostic quality. However, 80 kV in the overweight patients failed to produce images of diagnostic quality. The radiation dose in the patients imaged with 80 kV was significantly decreased in comparison with those imaged with 100 kV. The effective dose was 0.36 ± 0.06 and 0.41 ± 0.05 mSv in the slender and normal weight patients imaged with 80 kV.

Head and neck CTA scanning with 80 kV, automatic tube current modulation, and AIDR 3D algorithm can produce high quality images with reduced radiation dose in slender or normal weight patients.

Abbreviations: AIDR = adaptive iterative dose reduction, BMIs = body mass indexes, CNR = contrast-to-noise ratio, CTA = computed tomography angiography, CTDI = CT dose index, DLP = dose-length product, FBP = filtered back projection.

Keywords: body mass index, computed tomography, iterative reconstruction, radiation dose

1. Introduction

Computed tomography angiography (CTA) is the first choice for diagnosing head and neck vascular diseases due to its non-invasiveness. However, it has been a concern that CTA may affect the lens and thyroid, which are sensitive to radiation. In addition, computed tomography (CT) examination has been associated with an increased risk of cancer.[1–4] Great endeavors have been taken to reduce the diagnostic radiation doses, including novel image reconstruction algorithms.

CT scans using the iterative reconstruction algorithm have superior image quality and lower radiation doses in comparison with the filtered back projection (FBP) algorithm.[5,6] The adaptive iterative dose reduction (AIDR) 3D algorithm, which is based on the raw data space and the image space, can minimize radiation dose by reducing tube voltage or current, without compromising image quality. It has been shown that the AIDR 3D algorithm is associated with high spatial resolution, less noise, and excellent images.[7,8] In head and neck CTA examinations, the scanning protocol of 80 kV plus AIDR 3D significantly increased vascular attenuation and contrast-to-noise ratio (CNR) in comparison with 120 kV plus FBP.[9,10] Another study showed that CTA with 100 kV plus AIDR 3D significantly reduced radiation dose by 71%.[11]

It has been shown that coronary CTA with lower tube voltage had reduced radiation dose in patients with normal body mass index (BMI).[12] Another study found that radiation dose was positively correlated with BMI in craniocervical CTA.[13] We speculate that BMI may be a factor for consideration in planning head and neck CTA protocols with lower radiation doses. Therefore, our present study aimed to compare CTA scans of 100 kV plus AIDR 3D with those of 80 kV plus AIDR 3D among patients with different BMIs.

2. Materials and methods

2.1. Patients

Our study was approved by the ethics committee of Cangzhou Central Hospital. Informed consent was obtained from all

Editor: Wilhelm Mistiaen.

SY and JZ have contributed equally to this work.

Our study was approved by the ethics committee of Cangzhou Central Hospital. Informed consent was obtained from all patients before the enrollment.

The authors have no conflicts of interest to disclose.

Department of Diagnostic CT, Cangzhou Central Hospital, Cangzhou, Hebei, China.

* Correspondence: Shujing Yu, Department of Diagnostic CT, Cangzhou Central Hospital, No. 16, Xinhua road, Cangzhou, Hebei 061001, China (e-mail: shujingyu_med@126.com).

Medicine (2018) 97:36(e11841)

Received: 7 May 2018 / Accepted: 20 July 2018

http://dx.doi.org/10.1097/MD.0000000000011841

patients before the enrollment. From November 2016 to January 2017, 128 consecutive patients scheduled for head and neck CTA examinations were prospectively enrolled in our study. Their primary symptoms include headache, dizziness, and numbness of the limbs. All the patients had no previous history of allergy to iodine or major organ insufficiency. The patients were randomized into the 100-kV group (n = 60) and the 80-kV group (n = 68). The patients were further grouped as slender (BMI $< 22\,kg/m^2$), normal weight ($22\,kg/m^2 \leq$ BMI $< 25\,kg/m^2$), and overweight (BMI $\geq 25\,kg/m^2$).

2.2. Scanning protocols

All CTA examinations were performed with an 80-row CT scanner (PRIME, Toshiba, Japan). The following scanning settings were used: collimator 80 × 0.5 mm, pitch 0.831:1, slice thickness 0.5 mm, slice gap 0.5 mm, gantry rotational speed 0.5 s/r, field of view 320 × 320 mm, and matrix size 512 × 512. Both groups used the automatic tube current modulation technique (40–600 mA), a noise index of 15.0, and the AIDR 3D algorithm. The scanning covered the length from the aortic arch to the cranial base with acaudal-to-rostral direction. The scanning was triggered by the automatic bolus tracking technique. The region of interest (ROI) included the descending aorta at the level of the aortic arch, with a triggering threshold of 160 HU. Iohexol 350 (60 mL, 320 mg iodine/1 mL) was infused at 4 mL/s, followed by a bolus injection of 40 mL normal saline infused at 4 mL/s. The acquired raw data were transferred to a Vitrea Fx workstation for image analysis and reconstruction.

2.3. Objective assessment of image quality

The attenuation and the standard deviation were measured in the axial images of 0.5 mm slice thickness for the following structures: the right common carotid artery and the sternocleidomastoid at the C7 level, the right carotid sinus and the sternocleidomastoid at the C4 level, the right internal carotid artery and the masseter at the C1 level, and the M1 segment of the right middle cerebral artery and the brain tissue. The arterial ROI was placed in the center of the vessel, occupying approximately 2/3 of the lumen. The plaques were avoided. The ROIs for the muscular tissues and the brain tissues were set as $45\,mm^2$, avoiding the artifacts. Upon arterial stenosis or occlusion, the contralateral artery or muscular/brain tissue was measured instead. The signal-to-noise ratio (SNR) and the CNR were calculated for the neck and the brain segments, respectively. The SNR/CNR was the mean value of the common carotid artery, the carotid sinus, and the internal carotid artery. SNR = mean vascular HU/mean image noise. CNR = (mean vascular HU – mean muscular/brain HU) / mean image noise. Mean image noise = (mean vascular image noise – mean muscular/brain image noise)/2.

2.4. Subjective assessment of image quality

Two radiologists with over 5 years of experiences in head and neck CTA reviewed the CT images. They were blind to the scanning protocols and the study design, but not to the patient information. The image quality was assessed using the axial images of 0.5-mm slice thickness and curved planar reformation/maximum intensity projection (CPR/MIP) images. The cerebral arteries were assessed for the segments of level 3 and above.

The vascular image quality was categorized as 1 of the 5 scores from 1 to 5: 5 points, the vessels were fully filled with uniform intravascular density and sharp vascular wall, no artifacts; 4 points, the vessels were fully filled with uniform intravascular density, slightly blurred vascular wall or mild artifacts; 3 points, the vessels were generally well filled with uneven intravascular density, slightly blurred vascular wall or mild artifacts, but the images were still assessable; 2 points; the vessels were poorly filled with uneven intravascular density, blurred vascular wall, and significant artifacts, and the assessment was limited; 1 point, the vessels were not recognizable with significant artifacts, and the diagnosis was not possible. Images with a score ≥3 were deemed of diagnostic quality, while those with a score ≤2 were deemed of non-diagnostic quality.

The quality of the brain tissue images was also categorized as 1 of the 5 scores from 1 to 5: 5 points, the subarachnoid space was clear with well demarcated gray/white matter, fine image particles, no artifacts; 4 points, the subarachnoid space and the gray/white matter demarcation were recognizable, and the image particles were evenly distributed but not fine, no significant artifacts; 3 points, the subarachnoid space and the gray/white matter demarcation were barely recognizable, and the image particles were unevenly distributed with mild artifacts; 2 points, the subarachnoid space and the gray/white matter demarcation were unrecognizable, and the images were slightly blurred with coarse particles; 1 point, the images were blurred with very coarse particles. Images with a score ≥3 were deemed of diagnostic quality, while those with a score ≤2 were deemed of non-diagnostic quality.

2.5. Radiation dose assessment

The dose-length product (DLP) and the CT dose index (CTDI) were obtained from the CT scanner. The effective dose was calculated using the formula: effective dose = DLP × K. The K was 0.0031 according to the European guidelines on quality criteria for CT.[14]

2.6. Statistical analysis

The continuous data were compared using the Student's *t*-test. The categorical data were compared using the chi-square test. The subjective scores of image quality were compared using the Mann–Whitney test. The interrater agreement was analyzed using the intraclass correlation coefficient. All statistical analyses were performed using the SPSS 19.0 software. $P < .05$ was considered statistically significant.

3. Results

There was no significant difference in gender, age, and BMI between the sub-BMI groups (all $P > .05$, Table 1).

3.1. Image quality

The 3 sub-BMI groups imaged with 80 kV had significantly higher attenuation, noise, SNR, and CNR of the neck vessels in comparison with those imaged with 100 kV (all $P < .05$). Whereas in terms of the head vessels, the 3 sub-BMI groups imaged with 80 kV had significantly higher attenuation and noise, but not SNR or CNR, in comparison with those imaged with 100 kV (all $P < .05$, Table 2).

Table 1

General information of the patients.

	100-kV group (n = 60)	80-kV group (n = 68)	Statistic	*P*-value
Slender (BMI < 22kg/m^2)				
n	19	21		
Age (year)	61.74 ± 9.15	58.62 ± 6.73	t = 1.049	.303
BMI (kg/m^2)	20.76 ± 1.28	20.35 ± 1.50	t = 0.838	.409
Male (n)	7	12	χ^2 = 1.648	.199
Normal weight (22 kg/m^2 ≤ BMI < 25 kg/m^2)				
n	22	23		
Age (year)	59.68 ± 12.76	58.52 ± 10.15	t = 0.338	.737
BMI (kg/m^2)	23.78 ± 0.73	23.58 ± 0.72	t = 0.913	.366
Male (n)	12	7	χ^2 = 2.680	.102
Overweight (BMI ≥ 25 kg/m^2)				
n	19	24		
Age (year)	59.16 ± 7.81	57.79 ± 10.09	t = 0.486	.630
BMI (kg/m^2)	28.46 ± 2.45	27.59 ± 4.80	t = 0.718	.477
Male (n)	14	15	χ^2 = 0.604	.437

BMI = body mass index.

All the sub-BMI groups either imaged with 100 kV or 80 kV, produced head and neck vessel images of diagnostic quality. The image scores of the common carotid artery of the slender, normal weight and overweight patients imaged with 80 kV were 4.46 ± 0.48, 4.15 ± 0.53, and 3.88 ± 0.56, respectively, showing a decreasing trend. There were significant differences in the brain tissue scores between the corresponding sub-BMI groups imaged with 100 kV and those imaged with 80 kV (all $P < .05$). The brain tissue scores of the slender, normal weight and overweight patients imaged with 80 kV were 3.31 ± 0.25, 3.02 ± 0.35, and 2.92 ± 0.32, respectively. However, the images of the slender and normal weight patients imaged with 80 kV were basically of diagnostic quality (Fig. 1). All the slender patients imaged with 80 kV had brain tissue scores of diagnostic quality. The brain tissue score was < 3 points in 3 normal weight patients (13.04%) and 5 overweight patients (20.83%) imaged with 80 kV, respectively (Table 3).

3.2. Radiation dose

The CTDI in the slender, normal weight and overweight patients imaged with 80 kV was significantly decreased by 15.17%, 18.29%, and 22.71%, respectively, in comparison with their corresponding sub-BMI groups imaged with 100 kV (all $P < .05$). Similarly, The DLP in the slender, normal weight and overweight patients imaged with 80 kV was significantly decreased by 15.42%, 20.61, and 21.71%, respectively, in comparison with their corresponding sub-BMI groups imaged with 100 kV (all $P < .05$). The effective dose was 0.36 ± 0.06, 0.41 ± 0.05, and 0.50 ± 0.06 mSv in the slender, normal weight, and overweight patients imaged with 80 kV (Table 4).

3.3. Interrater agreement

There was no significant difference in the intraclass correlation coefficient between the 2 radiologists ($P > .05$).

Table 2

Comparison of the attenuation, SNR, and CNR of the vessels.

	Slender (BMI < 22kg/m^2)		Normal weight (22 kg/m^2 ≤ BMI < 25 kg/m^2)		Overweight (BMI ≥ 25 kg/m^2)	
	Neck	Head	Neck	Head	Neck	Head
Attenuation (HU)						
100 kV	531.32 ± 49.24	485.12 ± 58.22	486.02 ± 80.04	449.37 ± 69.45	469.87 ± 86.25	444.59 ± 62.06
80 kV	729.27 ± 122.99	677.78 ± 96.73	651.13 ± 149.05	612.57 ± 144.68	643.69 ± 132.06	593.78 ± 119.36
t	−5.509	−7.042	−4.657	−4.856	−5.198	−5.287
P	< .0001	< .0001	< .0001	< .0001	< .0001	< .0001
Noise						
100 kV	14.82 ± 2.01	19.75 ± 3.44	14.84 ± 1.42	19.62 ± 3.01	15.35 ± 2.16	17.82 ± 2.99
80 kV	17.16 ± 0.91	23.64 ± 2.61	17.24 ± 1.57	22.73 ± 2.87	18.34 ± 1.90	21.95 ± 2.90
t	−4.463	−3.447	−5.386	−3.550	−4.828	−4.570
P	< .0001	< .0001	< .0001	< .0001	< .0001	< .0001
SNR						
100 kV	36.37 ± 5.17	25.42 ± 6.09	32.92 ± 5.54	23.18 ± 3.69	30.90 ± 5.33	25.42 ± 4.30
80 kV	42.65 ± 8.09	28.80 ± 3.67	37.90 ± 8.69	27.13 ± 6.07	35.19 ± 6.67	27.57 ± 5.89
t	−2.684	−1.783	−2.303	−2.622	−2.279	−1.331
P	.012	.085	.027	.012	.028	.191
CNR						
100 kV	32.00 ± 4.68	23.28 ± 5.60	28.67 ± 5.58	21.13 ± 3.47	26.70 ± 5.20	23.10 ± 4.02
80 kV	38.72 ± 7.89	27.09 ± 3.50	33.98 ± 8.80	25.27 ± 5.95	31.51 ± 6.77	25.62 ± 5.79
t	−3.026	−2.173	−2.431	−2.834	−2.552	−1.615
P	.005	.038	.020	.007	.015	.114

BMI = body mass index, CNR = contrast-to-noise ratio, SNR = signal-to-noise ratio.

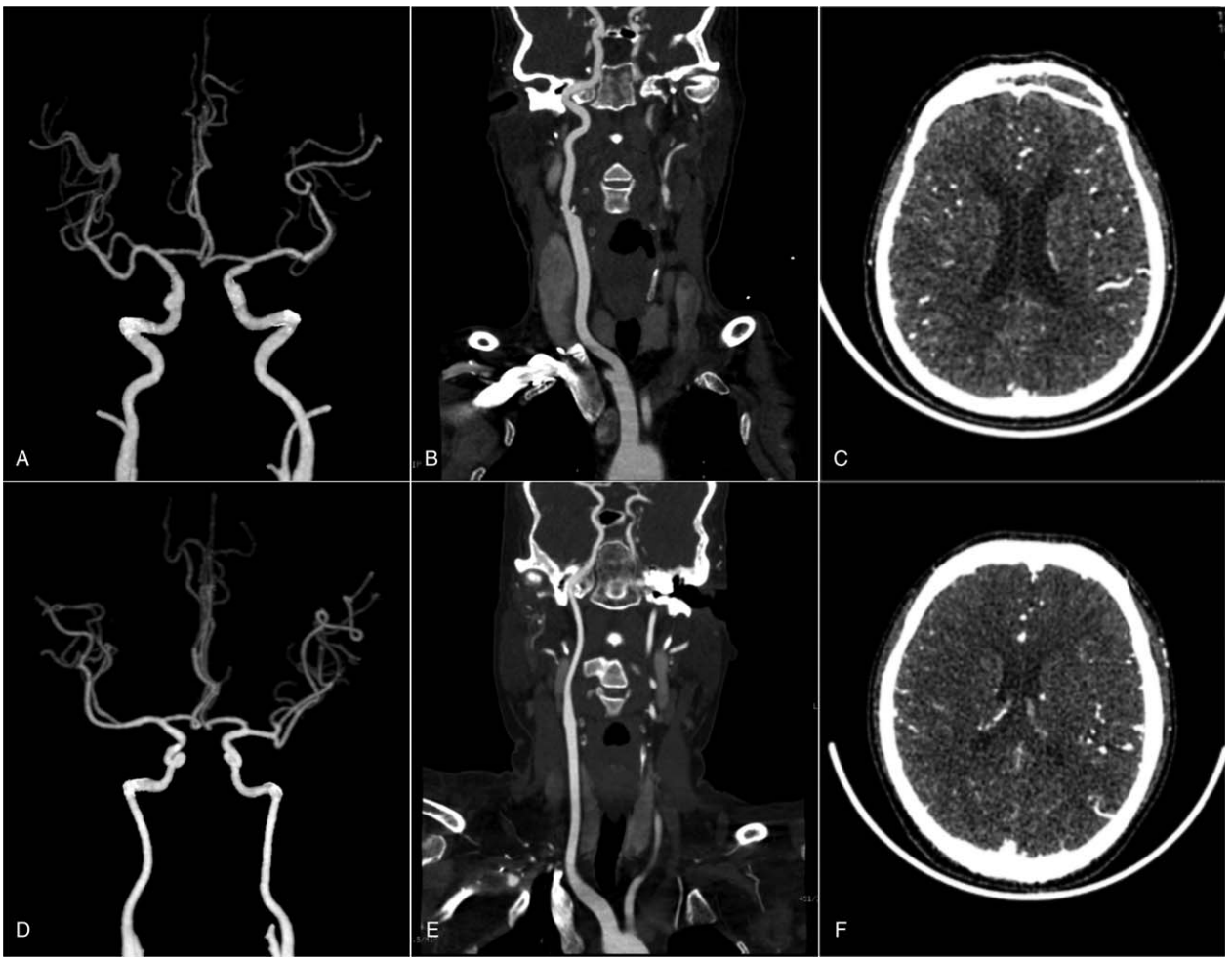

Figure 1. (A–C) A 57-year-old woman with a BMI of 23.55 was imaged with 100 kV. The subjective scores of her images were 4.83 for the neck vessels, 5.0 for the intracranial vessels, and 3.5 for the brain tissue. (D–F) A 55-year-old woman with a BMI of 24.32 was imaged with 80 kV. The subjective scores of her images were 4.83 for the neck vessels, 5.0 for the intracranial vessels, and 3.0 for the brain tissue. BMI = body mass index.

Table 3

Subjective scores of the image quality.

	100-kV group (n = 60)	80-kV group (n = 68)	*P*-value
Slender (BMI < 22kg/m^2)			
Right internal carotid artery at the C1 level	4.90 ± 0.27	4.77 ± 0.33	.305
Right carotid sinus at the C4 level	5.00 ± 0.00	5.00 ± 0.00	1.000
Right common carotid artery at the C7 level	4.63 ± 0.47	4.46 ± 0.48	.287
Right middle cerebral artery	4.66 ± 0.41	4.77 ± 0.39	.404
Brain tissue	3.68 ± 0.38	3.31 ± 0.25	.008
Normal weight (22 kg/m^2 ≤ BMI < 25 kg/m^2)			
Right internal carotid artery at the C1 level	4.77 ± 0.37	4.59 ± 0.39	.064
Right carotid sinus at the C4 level	5.00 ± 0.00	4.91 ± 0.25	.083
Right common carotid artery at the C7 level	4.55 ± 0.46	4.15 ± 0.53	.014
Right middle cerebral artery	4.36 ± 0.56	4.50 ± 0.66	.258
Brain tissue	3.52 ± 0.36	3.02 ± 0.35	.000
Overweight (BMI ≥ 25 kg/m^2)			
Right internal carotid artery at the C1 level	4.74 ± 0.42	4.56 ± 0.40	.118
Right carotid sinus at the C4 level	4.95 ± 0.16	4.92 ± 0.19	.568
Right common carotid artery at the C7 level	4.34 ± 0.55	3.88 ± 0.56	.012
Right middle cerebral artery	4.32 ± 0.45	4.40 ± 0.59	.429
Brain tissue	3.40 ± 0.52	2.92 ± 0.32	.002

BMI = body mass index.

Table 4

Radiation doses of the patients with different BMI.

	100-kV group (n = 60)	80-kV group (n = 68)	*t*	*P*-value
Slender (BMI < 22 kg/m^2)				
CTDI (mGy)	3.56 ± 0.85	3.02 ± 0.43	2.358	.026
DLP(mGy*cm)	137.85 ± 33.52	116.60 ± 19.18	2.273	.031
ED(mSv)	0.43 ± 0.10	0.36 ± 0.06	2.273	.031
Normal weight (22 kg/m^2 ≤ BMI < 25 kg/m^2)				
CTDI (mGy)	4.21 ± 1.12	3.44 ± 0.38	3.105	.005
DLP(mGy*cm)	166.42 ± 47.63	132.12 ± 15.25	3.223	.003
ED(mSv)	0.52 ± 0.15	0.41 ± 0.05	3.223	.003
Over weight (BMI ≥ 25 kg/m^2)				
CTDI (mGy)	5.24 ± 0.77	4.05 ± 0.42	6.049	<.0001
DLP(mGy*cm)	205.32 ± 31.27	160.74 ± 19.60	5.428	<.0001
ED (mSv)	0.64 ± 0.10	0.50 ± 0.06	5.428	<.0001

BMI = body mass index, CTDI = CT dose index, DLP = dose-length product, ED = effective dose.

4. Discussion

Our study showed that the images of the head and neck vessels or brain tissues in the sub-BMI patients imaged with 100 kV were of diagnostic quality. The slender and normal weight patients imaged with 80 kV also produced vascular and brain tissue images of diagnostic quality. However, only the head and neck vascular images were of diagnostic quality in the overweight patients imaged with 80 kV. These results suggested that BMI may affect the image quality during CTA scanning with 80 kV.

It has been shown that head and neck CTA scanning performed with 80 kV and AIDR 3D algorithm had significantly higher vascular attenuation and CNR and lower radiation doses in comparison with that performed with 120 kV and FBP algorithm.[9,10] However, these studies did not examine the brain tissue. Our findings confirmed the effectiveness of 80 kV and AIDR 3D in reducing CTA radiation doses in both vessels and brain tissues. The reduced tube voltage enhanced the contrast between the vessels and the adjacent structures, which resulted in higher vascular attenuation, noise, SNR, and CNR. This inhibited the effects of image noise and produced vascular images of high quality. However, the noise was not adequately inhibited due to the small disparity in brain tissue attenuation, despite the use of the AIDR 3D algorithm.

Yu et al showed that head and neck CTA with 100 kV plus AIDR 3D significantly reduced the radiation dose by 71% without compromising the image quality.[11] Inconsistent with the results of Yu et al,[11] our study showed that CTA scanning with 80 kV (plus automatic tube current modulation and AIDR 3D algorithm) in the slender and the normal weight patients can produce vascular images of high quality, in addition with the ability to assessing the brain tissue. The radiation dose in the patients imaged with 80 kV was significantly decreased in comparison with those imaged with 100 kV. The effective dose was 0.36 ± 0.06 and 0.41 ± 0.05 mSv in the slender and normal weight patients imaged with 80 kV.

In our study, the minimum vascular attenuation was near 600 HU, which is far beyond the optimal attenuation range for diagnosis (250–300 HU).[15] Excessively high attenuation can result in beam hardening artifact, which may compromise the accuracy in evaluating vascular plaques and stenosis. The high attenuation may be reduced by using a contrast of low concentration and a slower infusion rate.

In conclusion, head and neck CTA scan with 80 kV tube voltage, automatic tube current modulation, and AIDR 3D algorithm is recommended for patients with a BMI less than 25. This scanning protocol can produce vascular and brain tissue images of high quality, as well as lower radiation dose for better patient safety.

Author contributions

Conceptualization: Li Zhang.
Data curation: Jing Zheng.
Formal analysis: Li Zhang.
Methodology: Jing Zheng, Li Zhang.
Resources: Jing Zheng, Li Zhang.
Supervision: Li Zhang.
Validation: Shujing Yu, Jing Zheng.
Writing – original draft: Shujing Yu.
Writing – review & editing: Shujing Yu.

References

[1] Miglioretti DL, Johnson E, Williams A, et al. The use of computed tomography in pediatrics and the associated radiation exposure and estimated cancer risk. JAMA Pediatr 2013;167:700–7.
[2] Smith-Bindman R, Lipson J, Marcus R, et al. Radiation dose associated with common computed tomography examinations and the associated lifetime attributable risk of cancer. Arch Intern Med 2009;169:2078–86.
[3] Sodickson A, Baeyens PF, Andriole KP, et al. Recurrent CT, cumulative radiation exposure, and associated radiation-induced cancer risks from CT of adults. Radiology 2009;251:175–84.
[4] Berrington de Gonzalez A, Darby S. Risk of cancer from diagnostic X-rays: estimates for the UK and 14 other countries. Lancet 2004;363:345–51.
[5] Cho YJ, Schoepf UJ, Silverman JR, et al. Iterative image reconstruction techniques: cardiothoracic computed tomography applications. J Thorac Imaging 2014;29:198–208.
[6] Khawaja RD, Singh S, Gilman M, et al. Computed tomography (CT) of the chest at less than 1 mSv: an ongoing prospective clinical trial of chest CT at submillisievert radiation doses with iterative model image reconstruction and iDose4 technique. J Comput Assist Tomogr 2014;38:613–9.
[7] Wallihan DB, Podberesky DJ, Sullivan J, et al. Diagnostic performance and dose comparison of filtered back projection and adaptive iterative dose reduction three-dimensional ct enterography in children and young adults. Radiology 2015;276:233–42.
[8] Yoon JH, Lee JM, Hur BY, et al. Influence of the adaptive iterative dose reduction 3D algorithm on the detectability of low-contrast lesions and radiation dose repeatability in abdominal computed tomography: a phantom study. Abdom Imaging 2015;40:1843–52.
[9] Zhang WL, Li M, Zhang B, et al. CT angiography of the head-and-neck vessels acquired with low tube voltage, low iodine, and iterative image reconstruction: clinical evaluation of radiation dose and image quality. PLoS One 2013;8:e81486.
[10] Nakaura T, Nakamura S, Maruyama N, et al. Low contrast agent and radiation dose protocol for hepatic dynamic CT of thin adults at 256-

detector row CT: effect of low tube voltage and hybrid iterative reconstruction algorithm on image quality. Radiology 2012;264: 445–54.
[11] Yu S, Zhang L, Zheng J, et al. A comparison of adaptive iterative dose reduction 3D and filtered back projection in craniocervical CT angiography. Clin Radiol 2017;72:96.e1–6.
[12] Sun G, Hou YB, Zhang B, et al. Application of low tube voltage coronary CT angiography with low-dose iodine contrast agent in patients with a BMI of 26–30 kg/m2. Clin Radiol 2015;70:138–45.
[13] You J, Dai Y, Huang N, et al. Low-dose computed tomography with adaptive statistical iterative reconstruction and low tube voltage in craniocervical computed tomographic angiography: impact of body mass index. J Comput Assist Tomogr 2015;39:774–80.
[14] McCollough CH, Primak AN, Braun N, et al. Strategies for reducing radiation dose in CT. Radiol Clin North Am 2009;47:27–40.
[15] Ohnesorge BM, Hofmann LK, Flohr TG, et al. CT for imaging coronary artery disease: defining the paradigm for its application. Int J Cardiovasc Imaging 2005;21:85–104.